Matrix Completion for Direct Imaging of Exoplanets

Hazan Daglayan[1], **Simon Vary**[1], **Pierre-Antoine Absil**[1]
[1]ICTEAM, UCLouvain

Angular Differential Imaging (ADI)

When the light passes through the atmosphere, atmospheric turbulence deforms the signal of the planetary systems. This causes speckles which are very similar to the planets.

It is not possible to detect planets using only one image because of the speckles. As a result, multiple images of a star are taken through a night of observation, so the planets follow a circular trajectory.

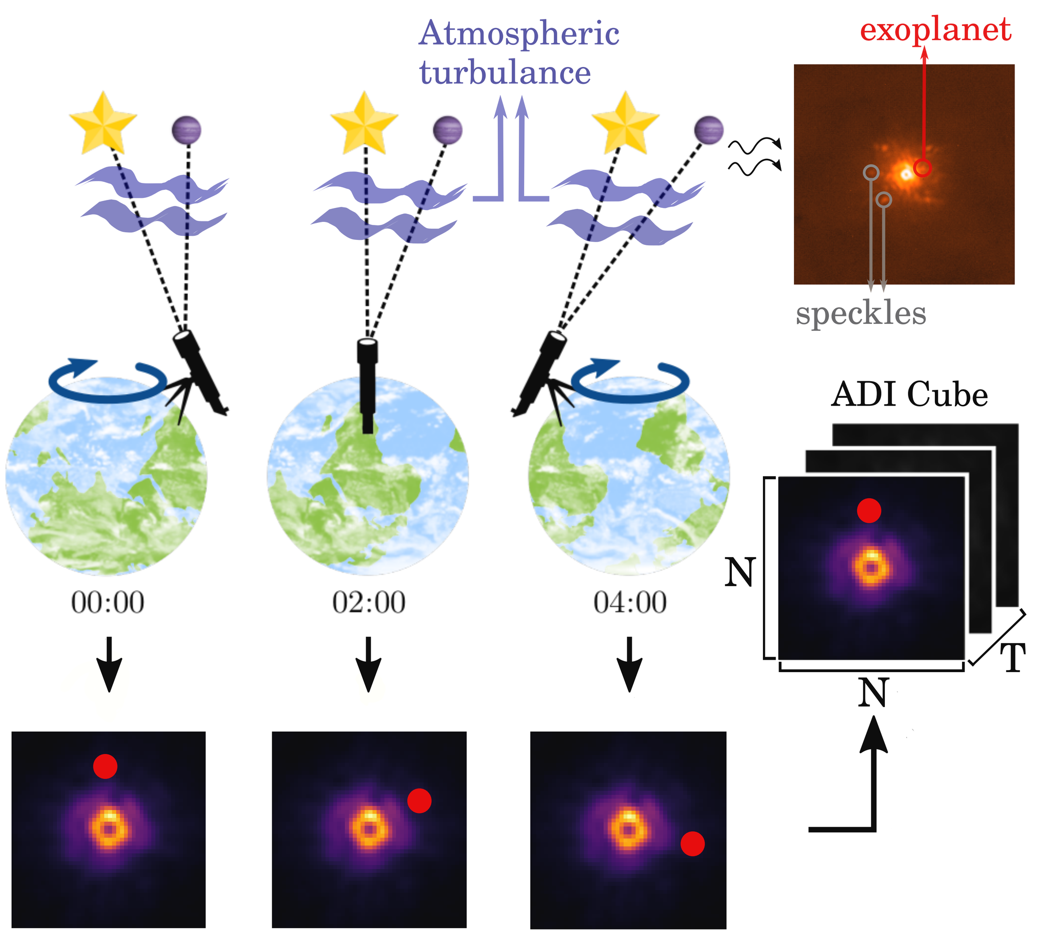

Principal Component Analysis (PCA)

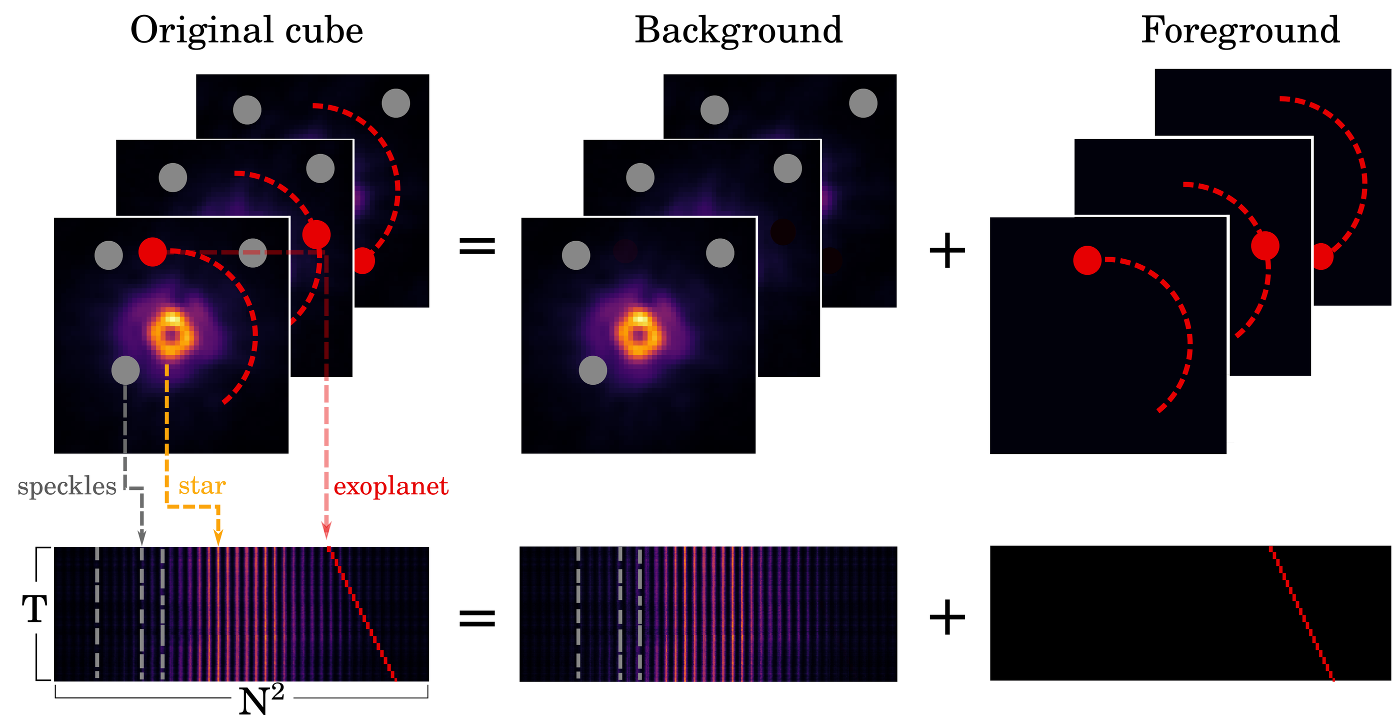

- Frames of the video sequence are stacked into $T \times N^2$ matrix.
- Low-rank PCA model approximates the static background. [1, 4]
- The residual matrix contains dynamic foreground, i.e. the planet.
- Derotation of the residual enhances even more the planet signal.

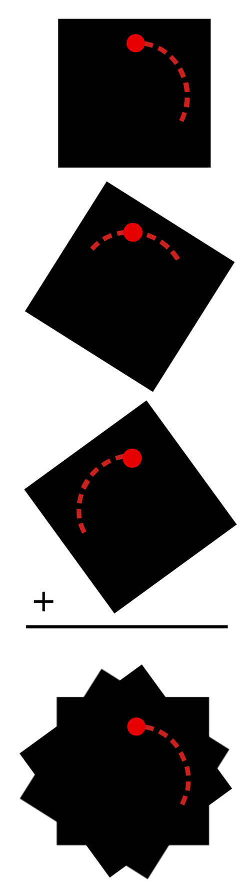

Matrix Completion for Exoplanet Detection (MC)

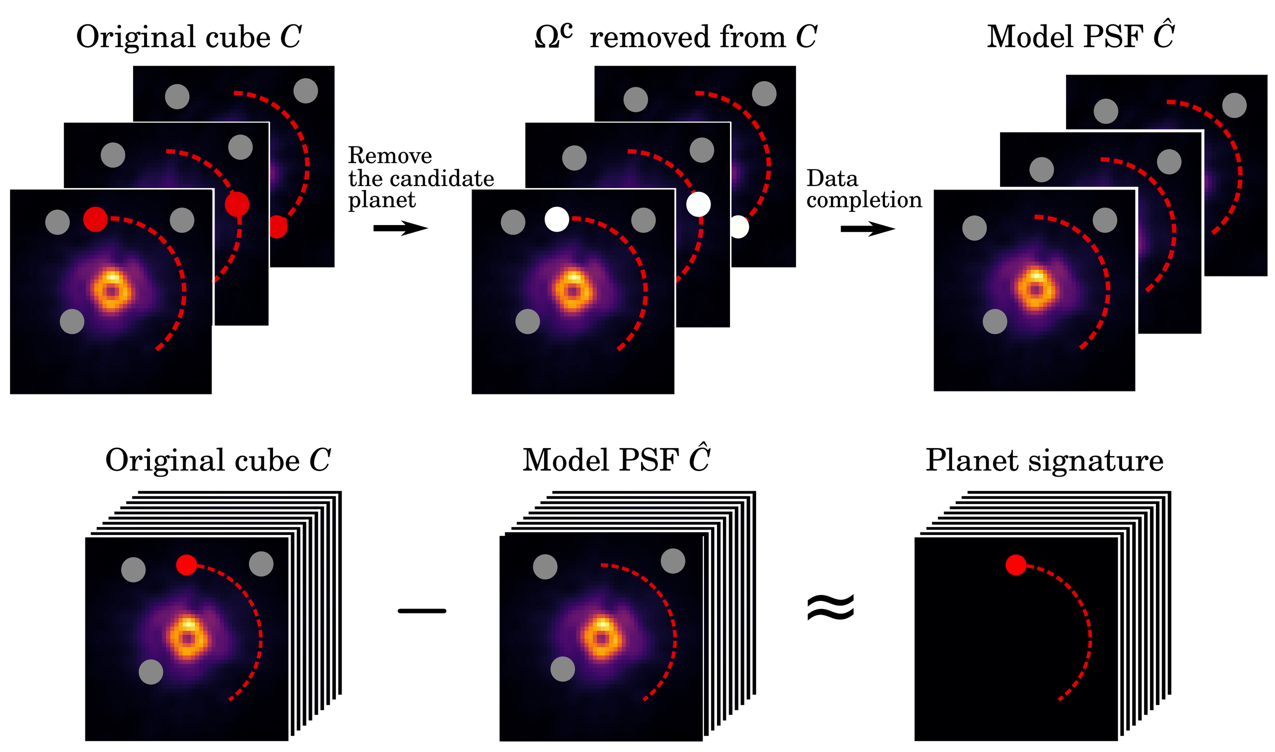

Shortcoming of PCA: The **low-rank approximation** can be affected by the moving planet resulting into **poorer detection**.

Proposed solution: Remove from the matrix pixels moving in time that correspond to the planet's trajectory and then approximate with a low-rank model. Since the trajectory of the planet is unknown, we try many different trajectories.

Algorithm 1 MC for Exoplanet Detection

1: **for each** pixel in the annulus **do**
2: Remove a trajectory centered a pixel (x_i, y_i).
3: Apply low-rank approximation with the trajectory missing.
4: Derotate the residual cube.
5: Assign the values of the derotated residual cube at pixels (x_i, y_i) to the final residual cube.
6: **end for**

Algorithm 2 Low-rank Matrix Fitting (LMaFit)[5]
Input: $P_\Omega(Z^0)$, $X_0 \in \mathbb{R}^{m \times r}$, $Y_0 \in \mathbb{R}^{r \times n}$

1: **repeat**
2: $X_{i+1} = Z_i Y_i^\dagger = \arg\min_X \|XY_i - Z_i\|_F^2$
3: $Y_{i+1} = X_{i+1}^\dagger Z_i = \arg\min_Y \|X_{i+1}Y - Z_i\|_F^2$
4: $Z_{i+1} = X_{i+1}Y_{i+1} + P_\Omega(Z^0 - X_{i+1}Y_{i+1})$
5: **until** termination criteria is reached

Likelihood Map

Assuming there is a planet along a trajectory g, the residual cube $R_g = C - \hat{C}_g$ is modeled as:

$$R_g = a_g P_g + N, \tag{1}$$

where $a_g > 0$ is the flux, P_g is the planet signature along g, and N is the residual noise. We can maximize the following log-likelihood to estimate the value of a_g

$$\log \mathcal{L}_g(a|R_g) \propto -\sum_{(t,r)\in\Omega_g{}^c} \frac{|R_g(t,r) - aP_g(t,r)|}{\sigma_{R_g}(r)}, \tag{2}$$

which models the residual error with a distribution that has an exponential decay as observed by [2].

Flux SNR Map

After the flux is approximated by maximizing (2) for each pixel in the annulus, we construct a frame of fluxes. Then, we compute the signal-to-noise ratio of the flux, S/N, by

$$S/N = \frac{a_g - \hat{a}}{s_a\sqrt{1 + \frac{1}{n}}} \tag{3}$$

where $\hat{a}$ and s_a are the mean and standard deviation value of fluxes for all the pixels and n is the number of elements at the same radial separation from the center.

Experiments

Real Dataset

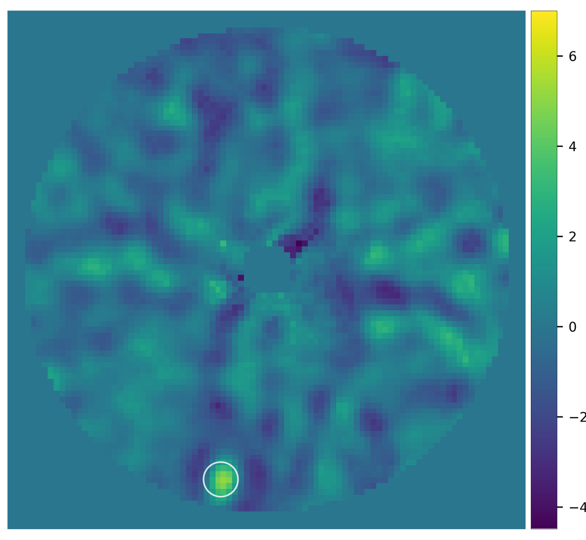
SNR after PCA

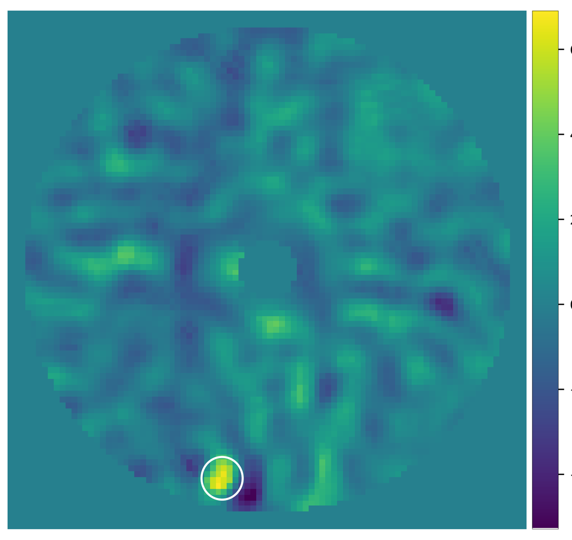
SNR after MC

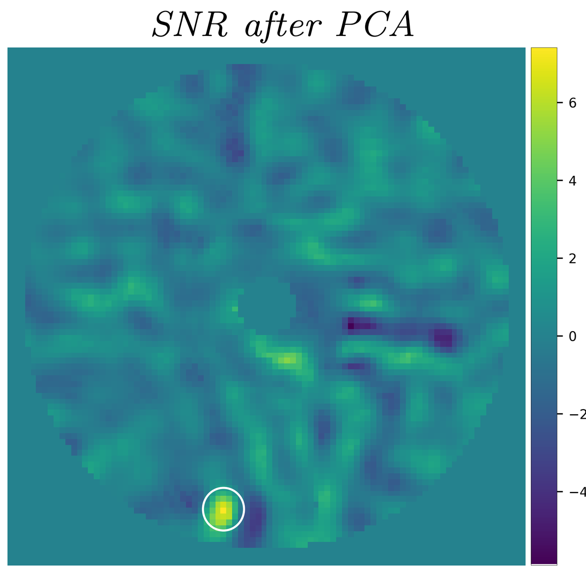
Flux SNR after MC

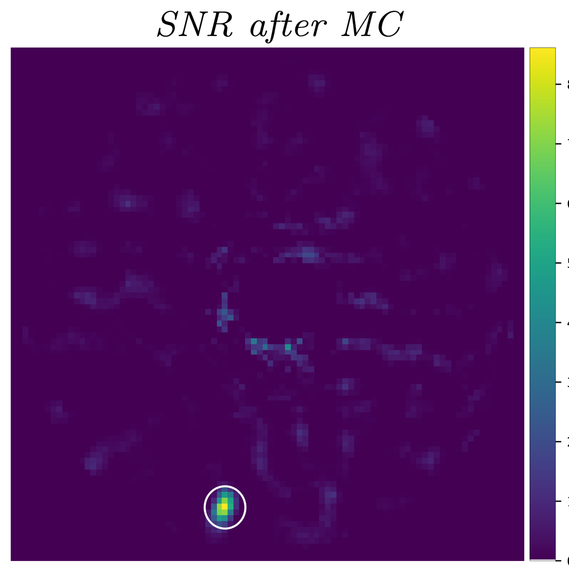
Likelihood after MC

Properties of the dataset and maps

- The ADI cube is VLT/SPHERE-IRDIS Eri in the K1 (2.11 μm) band.
- The dataset has 256 frames covering 42° and $\lambda/D \approx 4.9$ pixel [3].
- The real planet is on $7.7\lambda/D$ separation.
- We inject 4 planets on $2\lambda/D$, $5\lambda/D$, $8\lambda/D$, and $15\lambda/D$ separation.
- In detection maps, white circle represents the location of the planet.

Real planet: In real dataset results, all detection maps can detect the planet. However, the scales of the maps show that MC algorithms perform better.

Synthetic Planets: Only one of the planet is detected by PCA, while likelihood map after MC can detect all the planets. Moreover, the furthest planet from the star is best detected with SNR and Flux SNR maps after MC.

Synthetic Planets

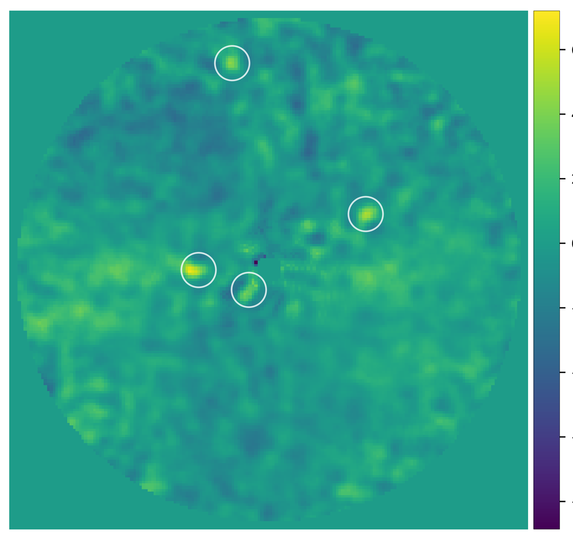
SNR after PCA

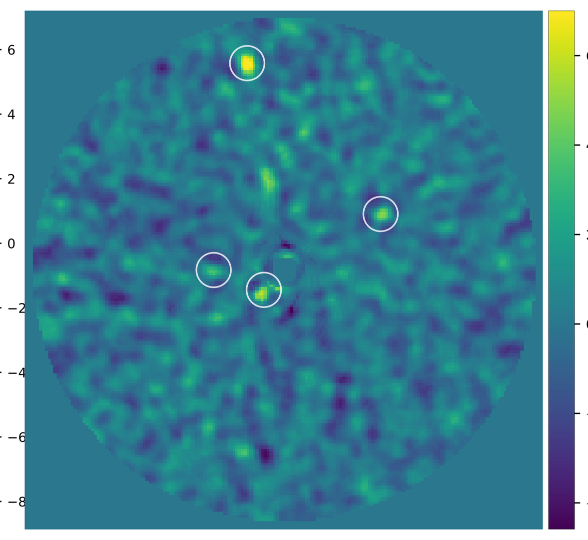
SNR after MC

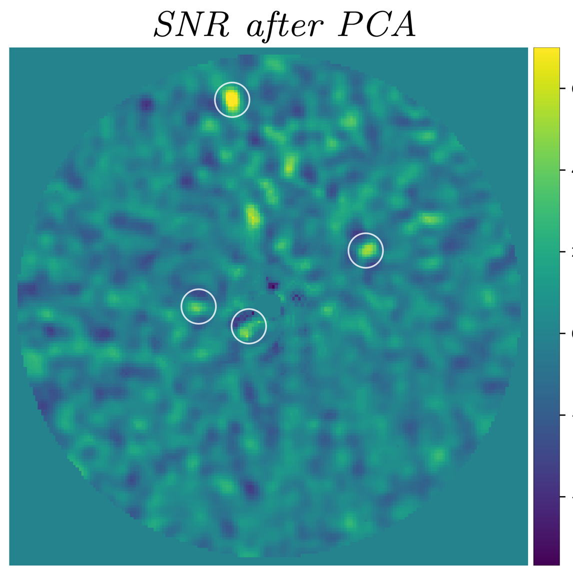
Flux SNR after MC

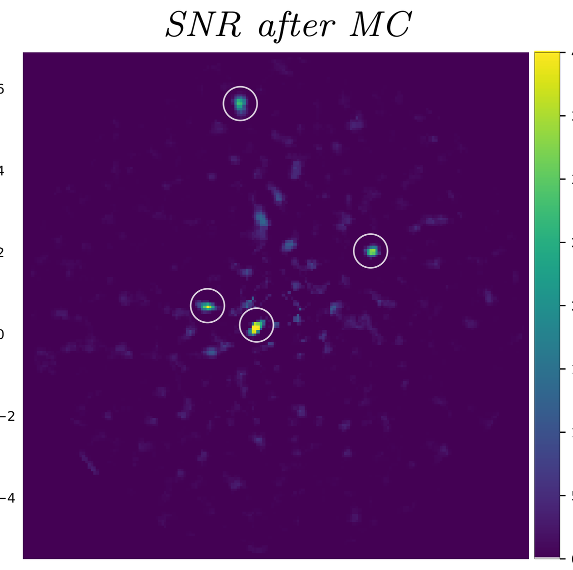
Likelihood after MC

References

[1] A. Amara and S. P. Quanz. Pynpoint: an image processing package for finding exoplanets. *Monthly Notices of the Royal Astronomical Society*, 427(2):948–955, 2012.
[2] B. Pairet, F. Cantalloube, C. A. Gomez Gonzalez, O. Absil, and L. Jacques. Stim map: detection map for exoplanets imaging beyond asymptotic gaussian residual speckle noise. *Monthly Notices of the Royal Astronomical Society*, 487(2):2262–2277, 2019.
[3] Samland, M., Mollière, P., Bonnefoy, M., Maire, A.-L., Cantalloube, F., Cheetham, A. C., Mesa, D., Gratton, R., Biller, B. A., Wahhaj, Z., Bouwman, J., Brandner, W., Melnick, D., Carson, J., Janson, M., Henning, T., Homeier, D., Mordasini, C., Langlois, M., Quanz, S. P., van Boekel, R., Zurlo, A., Schlieder, J. E., Avenhaus, H., Beuzit, J.-L., Boccaletti, A., Bonavita, M., Chauvin, G., Claudi, R., Cudel, M., Desidera, S., Feldt, M., Fusco, T., Galicher, R., Kopytova, T. G., Lagrange, A.-M., Le Coroller, H., Martinez, P., Moeller-Nilsson, O., Mouillet, D., Mugnier, L. M., Perrot, C., Sevin, A., Sissa, E., Vigan, A., and Weber, L. Spectral and atmospheric characterization of 51 eridani b using vlt/sphere. *A&A*, 603:A57, 2017.
[4] R. Soummer, L. Pueyo, and J. Larkin. Detection and characterization of exoplanets and disks using projections on karhunen–loève eigenimages. *The Astrophysical Journal Letters*, 755(2):L28, 2012.
[5] Z. Wen, W. Yin, and Y. Zhang. Solving a low-rank factorization model for matrix completion by a nonlinear successive over-relaxation algorithm. *Mathematical Programming Computation*, 4(4):333–361, 2012.